HHS Public Access

Author manuscript

Neurobiol Dis. Author manuscript; available in PMC 2021 May 01.

Published in final edited form as:

Neurobiol Dis. 2021 May ; 152: 105299. doi:10.1016/j.nbd.2021.105299.

Identification of protein quality control regulators using a *Drosophila* model of TPI deficiency

Stacy L. Hrizo[a,c], **Samantha L. Eicher**[a,b], **Tracey D. Myers**[a,b], **Ian McGrath**[a,b], **Andrew P. K. Wodrich**[a,b], **Hemanth Venkatesh**[a,b], **Daniel Manjooran**[a,b], **Sabrina Swoger**[a,b], **Kim Gagnon**[a,b], **Matthew Bruskin**[a,b], **Maria V. Lebedev**[a,b], **Sherry Zheng**[a,b], **Ana Vitantonio**[a,b], **Sungyoun Kim**[a,b], **Zachary J. Lamb**[a,b], **Andreas Vogt**[d], **Maura R.Z. Ruzhnikov**[e,f], **Michael J. Palladino**[a,b,*]

[a] Department of Pharmacology & Chemical Biology, University of Pittsburgh School of Medicine, Pittsburgh, PA 15261, USA

[b] Pittsburgh Institute for Neurodegenerative Diseases, University of Pittsburgh School of Medicine, Pittsburgh, PA 15261, USA

[c] Department of Biology, Slippery Rock University of Pennsylvania, Slippery Rock, PA 16057, USA

[d] Department of Computational & Systems Biology, Drug Discovery Institute, University of Pittsburgh School of Medicine, Pittsburgh, PA 15261, USA

[e] Department of Neurology, Stanford University School of Medicine, Stanford, CA 94304, USA

[f] Department of Pediatrics, Division of Medical Genetics, Stanford University School of Medicine, Stanford, CA 94304, USA

Abstract

Triosephosphate isomerase (TPI) deficiency (Df) is a rare recessive metabolic disorder that manifests as hemolytic anemia, locomotor impairment, and progressive neurodegeneration. Research suggests that TPI Df mutations, including the "common" TPI^{E105D} mutation, result in reduced TPI protein stability that appears to underlie disease pathogenesis. *Drosophila* with the recessive $TPI^{sugarkill}$ allele (a.k.a. *sgk* or *M81T*) exhibit progressive locomotor impairment, neuromuscular impairment and reduced longevity, modeling the human disorder. $TPI^{sugarkill}$ produces a functional protein that is degraded by the proteasome. Molecular chaperones, such as Hsp70 and Hsp90, have been shown to contribute to the regulation of $TPI^{sugarkill}$ degradation. In addition, stabilizing the mutant protein through chaperone modulation results in improved TPI deficiency phenotypes. To identify additional regulators of $TPI^{sugarkill}$ degradation, we performed a genome-wide RNAi screen that targeted known and predicted quality control proteins in the cell

* Corresponding author at: Department of Pharmacology & Chemical Biology, University of Pittsburgh School of Medicine, Pittsburgh, PA 15261, USA. mjp44@pitt.edu (M.J. Palladino).

Declaration of Competing Interest

The authors declare that they have no known competing financial interests or personal relationships that could have appeared to influence the work reported in this paper.

Supplementary data to this article can be found online at https://doi.org/10.1016/j.nbd.2021.105299.

to identify novel factors that modulate TPI^{sugarkill} turnover. Of the 430 proteins screened, 25 regulators of TPI^{sugarkill} were identified. Interestingly, 10 proteins identified were novel, previously undescribed *Drosophila* proteins. Proteins involved in co-translational protein quality control and ribosome function were also isolated in the screen, suggesting that TPI^{sugarkill} may undergo *co*-translational selection for polyubiquitination and proteasomal degradation as a nascent polypeptide. The proteins identified in this study may reveal novel pathways for the degradation of a functional, cytosolic protein by the ubiquitin proteasome system and define therapeutic pathways for TPI Df and other biomedically important diseases.

Keywords

Triosephosphate isomerase; TPI deficiency; Protein quality control; Proteasome; Molecular chaperone; Protein degradation; Polyubiquitination

1. Introduction

Triosephosphate isomerase (TPI) is a glycolytic enzyme that converts dihydroxyacetone phosphate to glyceraldehyde-3-phosphate. Numerous mutations affecting this enzyme are associated with a devastating recessive degenerative neuromuscular disorder called TPI Deficiency (TPI Df). Individuals homozygous for the "common" *TPI*^{E105D} allele or compound heterozygous with various alleles are affected. Patients typically exhibit childhood-onset hemolytic anemia, reduced immune function, progressive neuromuscular degeneration and premature death (Orosz et al., 2006). Data obtained with patient cells suggest that the missense mutations in the *TPI* gene produce enzymes that are less stable resulting in reduced TPI protein (Orosz et al., 2009). Currently there are no treatments for patients with TPI Df and the identification of novel pharmacological targets for the disorder would be beneficial in developing treatments.

Previously a *Drosophila* strain was isolated with a mutation in *TPI* called *sugarkill* that models TPI Df. *TPI*^{sugarkill} is recessive and in homozygotes causes TPI protein instability associated with progressive locomotor impairment, neurodegeneration and early death (Celotto et al., 2006; Seigle et al., 2008). Previous studies on these flies have found that the TPI^{sugarkill} protein is bound by the molecular chaperones Hsp70 and Hsp90 and is subsequently degraded by the proteasome (Hrizo and Palladino, 2010). In addition, this instability can be modulated pharmacologically by targeting the molecular chaperone Hsp90 or the proteasome leading to more mutant protein that improves animal phenotypes and survival (Hrizo and Palladino, 2010). We and others have argued stabilizing mutant TPI protein is a promising and viable therapeutic approach for TPI Df (Seigle et al., 2008; Hrizo and Palladino, 2010;Segal et al., 2019). Although there are several known drugs that modulate HSP70, HSP90 and the proteasome, thus far all the available drugs are exceptionally toxic and currently their clinical significance centers on their established toxicity and ability to sensitize cells to chemotherapies (Miyata, 2005; Taldone et al., 2008; Wang and McAlpine, 2015; Yuno et al., 2018). The proteasome together with promiscuous chaperones such as HSP70 and HSP90 regulate much of the proteome suggesting their inhibitors may never be viable for use as chronic therapies (Yuno et al., 2018).

The protein quality control (PQC) pathway in the endoplasmic reticulum has been well studied with a variety of endogenous substrates (recently reviewed by (Sun and Brodsky, 2019). However, PQC regulators within the cytosolic compartment are less well defined, especially for substrates that are not prone to aggregation. The TPI^{sugarkill} protein is a soluble, functional, non-aggregation prone, cytoplasmic protein that is targeted for degradation by the proteasome (Hrizo and Palladino, 2010) and its study may identify novel PQC mechanisms and regulators. Interestingly, both TPI^{sgk} and TPI^{E105D} have alterations affecting their dimer interface and both mutant proteins are temperature-sensitive and possibly thermolabile by an incompletely understood mechanism leading to increased rates of degradation when cells are exposed to heat stress (Rodríguez-Almazán et al., 2008). A newly identified and severe TPI Df allele, *TPI*^{R190Q}, has recently been described (Roland et al., 2019). Patient fibroblasts with this mutation exhibit extremely low TPI levels, and the patient has a clinical history of increasing severity of symptoms coincident with infections suggesting her severe symptoms may be febrile in origin (Roland et al., 2019). Our studies take advantage of the thermolabile nature of TPI Df mutant proteins using *TPI*^{sugarkill} to enable a powerful temperature-sensitive RNAi screen in *Drosophila*. We have performed a genome-wide RNAi screen of all known and predicted components of the UPS and PQC pathways and numerous unknown proteins with domains similar to those commonly found in UPS/PQC components. Importantly, the screen identified 25 proteins that are critical to TPI stability, including many that were not previously known to be involved in its turnover and novel proteins with no known or associated PQC function for *any* substrate. The screen independently identified several previously known factors involved in TPI degradation, substantiating these findings and suggesting that the screen likely identified the majority of regulators. Many of the novel PQC modulators are of “unknown function” and all of the identified proteins have a predicted human ortholog. Importantly, these potential regulators of mutant TPI are likely to be much less promiscuous than HSP70/HSP90, suggesting discovery of less toxic agents that stabilize mutant TPI is feasible.

2. Methods and materials

2.1. Strain information

Drosophila melanogaster with the following homozygous genotype: *w; DJ694-Gal4; GE-TPI*^{sgk}*e* were generated. The *GE-TPI*^{sgk} allele (also known as *TPI*^{sugarkill}) is a genomically engineered allele of *TPI* that only contains the single point mutation resulting in the M81T substitution (Roland et al., 2013). *Ebony* (*e*) is linked to the *TPI* locus and is used as a recessive marker. In all experiments, matings were performed to generate flies homozygous for *TPI*^{sugarkill} with the desired UAS-RNAi transgene and Gal4 driver. DJ694-Gal4 is a muscle driver that was used to drive the expression of the RNAi broadly in muscle tissues. Muscle was selected over brain or a ubiquitous driver due to the sensitive nature of the nervous system to imbalances in the PQC system and the more reliable effectiveness of RNAi in muscle (Elefant and Palter, 1999; DiAntonio et al., 2001; Andersen et al., 2012; Fernandez-Cruz et al., 2020). Thus, supressors that are not expressed in muscle cannot be identified by this method. Flies were mated with transgenic RNAi strains on the 1st or 2nd chromosome from the Vienna stock collection. Each RNAi target was selected by prediction through Flybase using Flymine v31.0 for a role in protein folding, degradation,

ubiquitination and other quality control related processes. Each line was given an R# to conceal the identity of the factor until after the analyses were completed. The stock numbers and all genes targeted are listed in Supplemental Table 3, which includes the available off-target information. Fly strains that utilized p-elements to disrupt gene expression were used for validation studies. Zuo1 overexpressing line was mated with GE-M81T TPI for examining $TPI^{sugarkill}$ levels in the presence of higher levels of this chaperone. The strains used in the validation studies are listed in Supplemental Table 4.

2.2. Analysis of TPI protein stability by Western blot

To induce $TPI^{sugarkill}$ protein instability, 3–5 day old adult flies were incubated at 29C for 48 h (unless otherwise noted). Thoraxes were dissected and three thoraxes per sample were ground with a pestle in 80uL of 2× SDS PAGE sample buffer (130 mM Tris (pH 6.8), 4% SDS, 4% beta-mercaptoethanol, 20 glycerol, 0.1% bromophenol blue) with the protease inhibitors: leupeptin (1μg/uL final concentration), pepstatin A (0.5μg/uL final concentration), and PMSF (100uM final concentration). The samples were heated to 96C for 3 min, and then centrifuged at 5000 ×*g* for 1 min to pellet the debris. Then 20uL of the samples were loaded and run on a 12% SDS PAGE gel and transferred to a PVDF (0.45 μm) membrane using a BioRad Semi-Dry Transfer System. Samples were blocked with Odyssey Blocking reagent (Thermofisher Scientific) for 30 min at room temperature and then incubated in anti-TPI (1:5000, rabbit polyclonal, FL249, Santa Cruz Biotechnology) and anti-beta-tubulin (1:1000, mouse monoclonal E7, Developmental Studies Hybridoma Bank) diluted in Odyssey block overnight at 4C. Membranes were then washed 6 times in PBST, for 5 min each. Following the wash, membranes were incubated 1–3 h in the dark at room temperature in secondary antibodies: Goat anti-mouse-IR-680 (1:20000, A21057, Molecular Probes) and Goat anti-mouse-IR-800 (1:20000, NC9209374, Fisher Scientific) in Odyssey blocking reagent with 0.1% Tween 20. Finally, membranes were washed in PBST in the dark for another 6 washes, each lasting 5 min. The TPI and Beta-Tubulin bands were visualized on the membrane using the Odyssey Licor System and were quantified using densitometry with Image J software (NIH).

2.3. RNAi screen data analyses

The relative change in protein levels in the RNAi activated samples were compared to relative protein levels remaining in an RNAi minus control at 29C (expected levels of TPI instability). Both the RNAi and no RNAi 29C samples were normalized to a 25C no RNAi control at 25C (stable levels of TPI) with an $n = 4–8$ for each RNAi transgene. The samples were averaged and a Student's *t*-test with Bonferroni post-test correction for multiple comparisons was used to compare the relative amount of protein in an RNAi treated sample at 29C to the corresponding 29C no RNAi *Drosophila* sample set using Prism (raw data and *p* value information is available in Supplemental Table 1). Those samples that had a p value of less than 0.05 in the first screen were then reevaluated through a second independent set of matings, sample collection and Western Blot analyses. Due to the large nature of the primary screen data set and the length of the data collection time period, an ANOVA was not possible with these data. The secondary validation screen blots were set up with paired controls to ensure the data could be analyzed for significance using a one-way ANOVA and a Dunnett's post-test (Supplemental Table 2). The samples that yielded a p value of <0.05 in

both rounds of screening are highlighted in yellow on Supplemental Table 2. Importantly, with a screen of this magnitude false-negative results due to ineffective RNAi, as well as false positives due to off-target RNAi, are possible. A STRING analysis was conducted on these genes to examine interactions reported through experimental analysis at https://string-db.org/. Human orthologs of the genes were identified by DIOPT v8.0 on Flybase.

2.4. Isolation and visualization of poly-ubiquitinated TPI

Conjugated anti-TPI resin was prepared with TPI antibody (FL249, Santa Cruz Biotechnology) and the Pierce co-immunoprecipitation kit. Homozygous *TPI*^{sugarkill} flies were fed 1 mg/mL MG132 (Sigma) on 10% sucrose for 24 h at 25 or 29C. Following incubation, flies were homogenized using a mechanical homogenizer in Pierce co-immunoprecipitation lysis buffer with Protease Inhibitor Mini-Tablets (Pierce), MG132 (0.1 mg/mL, Sigma) and NEM (1uM, Sigma). Protein concentration was determined by BCA assay (Pierce). The lysates (2 mg) were incubated on a rotator overnight at 4C with 100ul of the conjugated anti-TPI resin. The columns were washed three times with 200uL of Pierce IP wash buffer with Protease Inhibitor Mini-Tablets (Pierce), MG132 (0.1 mg/mL) and 1uM NEM. A bead only control provided by the Pierce IP kit served as a negative control. The samples were eluted into 2× SDS PAGE sample buffer (130 mM Tris (pH 6.8), 4% SDS, 4% beta-mercaptoethanol, 20 glycerol, 0.1% bromophenol blue) with Protease Inhibitor Mini-Tablets (Pierce), MG132 (0.1 mg/mL, Sigma) and NEM (1uM, Sigma). Western blots were conducted as described above with the exception that the blots were boiled in distilled water for 30 min prior to blocking for better detection of polyubiquitinated moieties as previously described (Ahner et al., 2007). The antibody used for detection of ubiquitin was anti-ubiquitin (1:1000, 6C1 mouse Santa Cruz Biotechnology). Ubiquitin bands were visualized on the membrane using the Odyssey Licor System.

2.5. Validation with classical mutant alleles

Validation of RNAi line results were conducted utilizing available p-element disruption strains and a GFP-tagged zuo1 overexpressing line (Supplemental Table 4). Validation included mechanical stress sensitivity analysis and life span analysis with flies homozygous for both the p element and the *GE-TPI*^{sgk} allele. Western blots were conducted as above, but at 25C for 5 days for the p-element disruption lines as high heat was lethal for many protein-quality control factor p-element disrupted lines. Results were compared by a One-way ANOVA (Prism). Mechanical stress sensitivity (a.k.a. bang-sensitivity), was performed on day 5 adults (aged at 25C). Animals were vortexed and observed for a return to normal behavior following paralysis and seizure, as has been previously described (Seigle et al., 2008). The average time to recovery was calculated and the data were examined for significance compared to *GE-TPI*^{sgk}*e* homozygote control using a One-way ANOVA (PRISM). For lifespan analysis, approximately 25 flies aged day 1 were isolated in a vial and were maintained at 25C. Animals were provided fresh media every 48 h and deaths were noted. Trials were run in triplicate. Mantel-Cox analysis using PRISM software was used to generate survival curves, determine median lifespan and evaluate significance.

2.6. Culturing patient fibroblasts

Patient fibroblasts were obtained from a male TPI deficiency patient via skin punch using Stanford University IRB (Registration 5135, e-protocol 28342, Dr. G. Enns). The cells were de-identified and are known only as FB104. Fibroblasts were cultured using standard methods (37C, 5% CO_2) in complete media (DMEM with 10% serum, 100 U penicillin/100 μg streptomycin/ml (Lonza), 2 mM L-glutamine (Gibco) and supplemental non-essential amino acids (Gibco).

2.7. Patient fibroblast Western blots

Human fibroblasts were treated with Luminespib (200 nM, Selleck Chemicals) and DMSO (0.1%, Sigma Aldrich), then incubated at standard conditions (37C, 5%CO) for 48 h. Cells were then trypsinized (0.05% for 5 min), pelleted, resuspended in RIPA buffer with protease inhibitors (PMSF (100uM), Leupeptin (1 μg/uL), Pepstatin A (0.5 μg/uL)) and were pulse sonicated. Protein concentrations were determined using a BCA assay (Pierce). Immunoblotting was performed on whole protein cell lysates following the addition of an equal volume of 2× SDS PAGE sample buffer (4% SDS, 4% β-mercaptoethanol, 130 mM Tris HCl pH 6.8, 20% glycerol). Proteins were resolved by SDS-PAGE (12%), transferred onto 0.45 μm PVDF membrane. The blots were blocked in Odyssey Blocking Buffer (Licor) and incubated with anti-TPI (1:5000; rabbit polyclonal FL-249; Santa Cruz Biotechnology) or anti-Beta-tubulin (1:1000; mouse polyclonal E7-C; Developmental Studies Hybridoma Bank) diluted in Odyssey Blocking Buffer (Licor). Following washes in PBST, the blots were incubated with anti-mouse-IR800 (Fisher Scientific) and anti-rabbit-IR680 (Molecular Probes) both diluted to 1:20,000 in 0.1% Tween 20 blocking buffer. Blots were washed in PBST and developed using Odyssey Infrared Imaging System. Quantification of the scanned images was performed digitally using the Image Studio Ver 5.2 software. Differences in TPI levels were evaluated for significance by a two-tailed Student's *t*-test.

3. Results

3.1. Primary genetic screen

The initial RNAi screen evaluated the expression of 430 different Gal4-dependent UAS-RNAi constructs targeting the expression of a variety of known or predicted protein quality control factors in *Drosophila*. The initial screening yielded a total of 95 factors that were involved in $TPI^{sugarkill}$ degradation using a Bonferroni correction for multiple comparisons (significant p value of <0.00011). Of the 430 RNAi lines tested 217 were reduced with a $p<0.05$ (without multiple comparison correction (Supplemental Table 1). The knock down of these factors generally resulted in increased stabilization of $TPI^{sugarkill}$ compared to corresponding controls with no RNAi, treated at 29C. Each RNAi data set was compared to the equivalent 29C control. A representative Western blot is shown in Fig. 1A with analysis in Fig. 1B. The no RNAi, DJ694 GAL4 driver line expressing $TPI^{sugarkill}$ demonstrated significant degradation of the $TPI^{sugarkill}$ protein following incubation at 29C for 48 h compared to flies of the same genotype incubated at 25C for 48 h. The level of degradation in the control lines was consistent with previously published data that demonstrated ~60–70% reduction in protein levels (Seigle et al., 2008; Hrizo and Palladino, 2010). The RNAi strains expressing $TPI^{sugarkill}$ were also incubated at 29C for 48 h and the relative amount of

TPI protein remaining was compared to the 29C no RNAi control on the same blot. This allowed the researchers to account for blot variability. Beta-tubulin was used as a loading control for all Western blots as the levels of beta-tubulin were robust and stable under the conditions tested.

3.2. Secondary RNAi screen

To be inclusive in the second round of screening, the 217 lines identified as potential factors involved in regulating $TPI^{sugarkill}$ degradation (Fig. 1C and Supplemental Table 1) were re-evaluated through a second round of crosses and Western blot analyses. This analysis yielded 25 lines that were significantly different compared to the no RNAi treated samples at 29C when examined by a One Way Anova with a Dunnett's Post Test ($p<0.05$) (Fig. 2 and Table 1). Interestingly, there were several expected hits identified by the screen such as Hsp70 and Hsp83. Both have been previously shown to regulate $TPI^{sugarkill}$ degradation (Hrizo and Palladino, 2010).

3.3. STRING analysis of regulators

Interestingly, our screening suggests $TPI^{sugarkill}$ degradation is regulated by 10 novel/uncharacterized proteins that are predicted to function in protein quality control and processing. These include putative chaperones, proteases, polyubiquitination enzymes and ribosome associated factors. String analyses use freely available protein-protein interaction data collected from reported experimental evidence in literature and computational prediction methods to generate the node diagram. Thicker lines shown in the STRING analysis indicate multiple levels of support for the reported interactions suggesting that these interactions are highly likely to be valid (Fig. 3). There were 3 main interconnected nodes identified in the analysis, molecular chaperones, ubiquitination and proteasome function and a minor unconnected mitochondrial node. As the protein quality control system is highly redundant with many isoforms of the same chaperone and ubiquitination enzyme, it was expected that some classes of chaperones and factors may be enriched if they shared overlapping function. When an interaction map was generated using STRING, the genes identified in our screen appear to strongly cluster together according to function (Fig. 3). There is a clear node in the interaction map that contains molecular chaperone and factors associated with regulating chaperone function. The chaperone data set appears to be enriched for the Hsp20, Hsp40, Hsp70 and Hsp90 families of proteins. Based on this analysis, two known primary regulators of the Hsp90–70 cycle may be of interest in future studies of TPI folding and degradation. HoP was identified in the initial round of screening but failed to be significant following the more rigorous ANOVA statistical analysis, suggesting it may not have a significant role in $TPI^{sugarkill}$ protein turnover or we were unsuccessful at robustly knocking down this co-chaperone with RNAi. HiP was unable to be included in the initial screen because a target RNAi line on the 1st or 2nd chromosome was not available when the screen was initiated. Further experiments with classical alleles to see if the canonical HoP, HiP, Hsp70, Hsp90 folding pathway applies to $TPI^{sugarkill}$ may yield additional points of quality control inhibition for therapeutic targeting (Pratt and Dittmar, 1998; Cox and Johnson, 2011).

In addition to redundancy in the chaperone network, it is also known that there are often multiple E2 and E3 ubiquitination enzymes that target the same substrate (Chan et al., 2000; Stewart et al., 2016; Chinen and Lei, 2017; Zheng and Shabek, 2017; Hunt et al., 2019). This redundancy has been observed for some ER PQC ubiquitination proteins, such as Ubc6 and Ubc7 (Rubenstein and Hochstrasser, 2010). Therefore, it was not surprising to identify a node in the interaction map that is enriched for factors such as E2 ubiquitin conjugating enzymes, E3 ubiquitin ligases, and deubiquitinating enzymes as having a role in TPI^{sugarkill} stability. It will be interesting to see which of these factors coordinate their actions together in the targeting of a non-aggregation prone cytoplasmic protein.

3.4. Mutant TPI polyubiquitination

Importantly, this suggests that TPI^{sugarkill} undergoes polyubiquitination prior to degradation. To test this prediction, an immunoprecipitation and Western blot experiment was conducted to isolate and visualize polyubiquitinated TPI^{sugarkill}. As can be seen in Fig. 4, when treated with MG132, isolated TPI^{sugarkill} from fly extract exhibited an accumulation of polyubiquitinated signal. The bead only control did not exhibit any TPI signal or the characteristic high molecular weight, incompletely separated products typically associated with polyubiquitination. Polyubiquitinated TPI^{sugarkill} was observed at both 25 and 29C. This is not unexpected as even TPI^{sugarkill} flies incubated at 25C exhibit reduced TPI levels compared to flies expressing the wildtype TPI protein (Seigle et al., 2008; Hrizo and Palladino, 2010). MG132 treatment was used to help stabilize both samples prior to immunoprecipitation. MG132 treatment is fed to the flies and does not rescue protein levels back to wildtype levels. Therefore, this assay allowed for a qualitative detection of polyubiquitinated material, but the quantitative levels were not able to be assessed. It is important to note, wildtype TPI was not evaluated as the experimental focus was related to the pathogenic mutant TPI. Thus, it is not known if this is a feature unique to the TPI^{sugarkill} mutant protein.

3.5. Validation of select mutant TPI regulators

In order to validate factors identified in the RNAi screen, a select group of target genes were evaluated using available p-element disruptions or overexpression alleles in *TPI^{sugarkill}* homozygotes (strain information in Supplemental Table 4). The effect of knock down on gene function by p-element or gene overexpression was evaluated by Western blot, lifespan and mechanical stress sensitivity analyses. P-element disruption is systemic and is expected to knock down/out the targeted protein in all tissues. This had an effect on the overall health of the *TPI^{sugarkill}* flies, especially at elevated temperatures. Thus, many of the studies with p-element disruptions were conducted at 25C, where the animals exhibit a modest but significant reduction in protein levels compared to the wildtype control. The investigation of exacerbated proteolysis due to chronic exposure to 29C heat stress was not possible due to high death rates in the p-element fly population. Selected for the p-element disruption study were Hsp83 (a known regulator of TPI^{sugarkill} degradation), Cullin 3 (novel putative regulator involved in polyubiquitination identified in the screen) and HiP (a regulator of Hsp90 unable to be tested in the primary screen, but of interest due to the repeated identification of Hsp90 and Hsp70 as factors involved in TPI^{sugarkill} degradation) (Pratt and Dittmar, 1998; Hrizo and Palladino, 2010; Cox and Johnson, 2011; Genschik et al., 2013).

As shown in Fig. 5A, gene disruption alleles of *HIP*, *HSP90* and *cullin3* all resulted in modest increases in TPI^{sugarkill} protein levels at 25C. Raw Western blot data is available as Supplemental Fig. 1. Importantly, this improvement in protein levels also correlated to an improvement in recovery from paralysis following mechanical stress for all three alleles (Fig. 5B) and increased lifespan compared to the *TPI^{sugarkill}* homozygote control (Fig. 5C and D). It should be noted that even though the Cullin 3 rescue was modest, it resulted in a large very significant change in the behavioral phenotypes of the flies. In contrast, Hsp90 had a significant improvement in TPI^{sugarkill} protein levels but had the most modest improvement in behavior. This suggests that there are additional pathways that may be altered by these factors that are affecting neuronal health in the flies. The median lifespan of *TPI^{sugarkill}* flies at 25C is 7.5 days, but the modest increases in protein levels resulting from the p-element disruption was sufficient to increase the median lifespans to 14 days (Cullin 3), 12 days (HiP) and 11 days (Hsp90, not shown) with a p value of <0.001 for all analyses. This suggests that modulating the activity of these target genes results in an improvement in overall function and lifespan in this TPI deficiency model.

3.6. Possible co-translational regulation of mutant TPI

Another set of factors of interest identified by the screen were ribosome associated proteins, including Hsp40, Zuo1/DNAJC2 and CG5116. Zuo1 is found in the Ribosome Associated Chaperone (RAC) complex and assists with the folding of nascent polypeptides as they are synthesized by the ribosome (Amor et al., 2015; Zhang et al., 2017). It has been shown that the RAC is involved in targeting nascent polypeptides to be degraded co-translationally (Bengtson and Joazeiro, 2010; Brandman et al., 2012; Defenouillere et al., 2013; Lyumkis et al., 2014). As the levels of total TPI^{sugarkill} protein continue to destabilize over long periods of time following a shift to 29C, it is possible that this substrate may be targeted by the RAC for degradation co-translationally (Hrizo and Palladino, 2010). Due to lethality, a *zuo1* p-element disruption line was not able to be used for these studies (data not shown). However, flies with an additional copy of *zuo1* inserted into the chromosome which results in zuo1 overexpression was able to be utilized (Kudron et al., 2018). When zuo1 was overexpressed in *TPI^{sugarkill}* flies, the stability of the protein was decreased further and corresponded to a worsening of lifespan, suggesting an important role for this chaperone in modulating the protein levels of TPI^{sugarkill} (Fig. 6). Additional research is needed to understand the role of the RAC complex and confirm whether there is co-translational degradation of TPI.

3.7. Mutant TPI^{E105D} protein is reduced in patient fibroblasts

One diagnostic hallmark of TPI Df is a reduction in TPI activity that is almost always first discovered by measuring TPI activity from a blood sample. We and others have shown that pathogenesis and the reduced activity observed in blood samples in TPI Df patients is tied to reductions in TPI protein due to its reduced stability (Roland et al., 2019; Orosz et al., 2006). Using patient fibroblasts with the homozygous common mutation we've investigated TPI levels by Western blot as an indicator of protein stability. Our results demonstrate a ~ 40% reduction in TPI protein relative to the B-tubulin loading control in patient versus control fibroblasts (Fig. 7). *TPI$^{E105D/E105D}$* (FB104) cells have 0.6252 (SEM = 0.05952) relative TPI compared to 1.0 for the normalized control fibroblast levels or a 37.5% decrease in TPI protein. These results are consistent with previously published data on *TPI^{E105D}* suggesting

that the mutant protein is temperature-sensitive and has reduced stability due to proteolysis (Torres-Larios, 2008; De La Mora-De La Mora et al., 2013).

3.8. Elevation of TPI in patient cells with drug treatment

As reduced stability of TPI protein underlies TPI Df pathogenesis and mutant proteins retain activity, altering the turnover of mutant TPI protein may be of therapeutic value. As reduced protein stability has been observed in numerous pathogenic variants of TPI Df including the common mutation, such an approach could be broadly beneficial to TPI Df patients. In this and previous studies in flies, when Hsp90 levels were decreased with RNAi or p-element disruption, the result is an increase in $TPI^{sugarkill}$ levels (Hrizo and Palladino, 2010). Therefore, if the role of Hsp90 in TPI protein stability translated to human cells, a corresponding increase in TPI^{E105D} levels was expected in response to decreased Hsp90 activity due to pharmacological inhibition. For these studies, $TPI^{E105D/E105D}$ patient fibroblasts (FB104) were examined for changes in TPI protein steady state levels in response to treatment with the Hsp90 inhibitor Luminespib for 48 h. As expected, a corresponding increase in TPI^{E150D} stability was observed in response to treatment with the Hsp90 inhibitor (Fig. 8). $TPI^{E105D/E105D}$ (FB104) cells treated with 200uM Luminespib have relative TPI protein levels of 1.425 (SEM = 0.11) compared to 1.043 (SEM = 0.05) for DMSO-treated cells or a 36.6% increase in mutant TPI protein levels. This suggests that the chaperones and quality control factors identified in *Drosophila* may yield additional targets for development of TPI deficiency therapeutic treatments in the future.

4. Discussion

TPI Df is a devastating recessive disease with early childhood-onset that is caused by numerous missense mutations in the *TPI1* gene. Studies using patient cells as well as research in *Drosophila*, suggest that pathogenesis is driven by mutations that destabilize the protein (Torres-Larios, 2008; De La Mora-De La Mora et al., 2013; Seigle et al., 2008; Hrizo and Palladino, 2010; Roland et al., 2013; Roland et al., 2019; Orosz et al., 2006). Additionally, mutations in *TPI* that reduce catalytic activity are generally well-tolerated in mice as long as activity isn't completely abrogated and the resulting protein exhibits normal stability (Segal et al., 2019). Collectively these data have led us and others to argue that stabilizing mutant TPI protein is the most promising therapeutic approach for TPI Df (Seigle et al., 2008; Hrizo and Palladino, 2010; Segal et al., 2019). Previous work has demonstrated that mutant TPI is degraded by the proteasome in a chaperone-dependent manner (Celotto et al., 2006; Seigle et al., 2008; Hrizo and Palladino, 2010). Specifically, the role of Hsp70 and Hsp90 in $TPI^{sugarkill}$ degradation has been elucidated, and impairing this degradation led to improvements in progressive neurodegenerative phenotypes (Hrizo and Palladino, 2010). Existing compounds that target Hsp70 and Hsp90 have been evaluated for treatment of protein folding disorders such as cystic fibrosis and various types of cancer (Brodsky and Chiosis, 2006; Murphy, 2013; Wang and McAlpine, 2015; Ihrig and Obermann, 2017; Yuno et al., 2018). However, Hsp70 and Hsp90 are highly and ubiquitously expressed, promiscuous chaperones that regulate numerous important cellular processes and their inhibitors have the potential for significant side effects (Miyata, 2005; Taldone et al., 2008; Yuno et al., 2018). Identifying more specific regulators of TPI degradation may allow for a

combinatorial therapy to be developed that will aid in reducing the degradation of TPI, with less toxicity.

The goal of the RNAi screen was to identify novel factors that may impact the degradation of mutant TPI, in particular proteins other than HSP70 and HSP90. TPI^{sugarkill} is a relatively unique protein quality control substrate; it is an endogenous mutant protein that is structurally normal, functional and not aggregation prone, yet is still identified by the quality control system of the cell and targeted for proteasomal degradation (Seigle et al., 2008; Hrizo and Palladino, 2010; Roland et al., 2013). Therefore, the regulatory network involved in mutant TPI degradation, particularly those proteins that are more selective for mutant TPI, may be ideal targets for pharmacological intervention as potential therapies for TPI deficiency. The screen identified 25 potential targets for pharmacological research including the ubiquitination pathway, Hsp20 and the RAC complex. Studies are ongoing in many areas of protein quality control regulators and thus compounds discovered in other studies may also be rich sources for TPI deficiency treatment (Mattern et al., 2012; Landré et al., 2014). In addition, the kinetics of TPI^{sugarkill} protein degradation should be evaluated to determine if it is co-translational, post-translational or both. If the protein is primarily targeted for degradation in a co-translational manner, focusing on the early steps of recognition for proteolysis may be important in the development of future therapies.

Mitochondrial dysfunction has been implicated in a multitude of myodegenerative and neurodegenerative diseases, and it seems that mitochondrial health appears to play an important role in TPI deficiency. Previous work identified mitochondrial generated oxidative stress as a contributor to the neurological phenotypes observed in *TPI^{sugarkill}* flies (Hrizo et al., 2013). The screen did identify three proteins (CG32727, CG4164, and MGE) associated with mitochondrial function and it may be of interest to determine the mechanism by which the down regulation of these factors results in TPI stability. Importantly, modulation of oxidative stress by diet, such as the ketogenic diet, and by pharmacological methods such as reducing agents have been shown to improve phenotypes associated with metabolic mutations in flies (Hrizo et al., 2013; Fogle et al., 2016; Fogle et al., 2019). This suggests that compounds that modulate mitochondrial function and redox stress may also be of interest in developing a treatment strategy for TPI deficiency patients.

Importantly, preliminary studies in our lab with cell lines derived from *TPI^{E105D}* patients suggest that the TPI^{E105D} protein has lower steady state levels suggesting it too is unstable (Fig. 7) and the reduced TPI protein levels can be “rescued” with an Hsp90 inhibitor (Fig. 8). Of course, a 36.6% increase in a protein that is decreased 37.5% from that of wild type does not bring protein levels back to completely normal levels. Such an increase would return TPI protein levels to ~ 85% of their normal or wild type levels ((1.366 × 0.625) x 100% = 85.38%). Although this is not considered a complete “rescue”, such an improvement would be predicted to be of immense therapeutic value. Therefore, these data serve as proof-of-concept using patient cells that inhibiting the degradation pathway of mutant TPI protein could be beneficial as a therapeutic approach for TPI Df treatment. We are not suggesting that Luminsepib or other HSP90 inhibitors would make viable TPI Df treatments as they are generally not tolerated well and the ones tested so far do not have a toxicity profile needed for a chronic treatment in humans. However, several of the other proteins identified in this

screen, as putative modulators of mutant TPI turnover, are likely much less promiscuous (e.g. more selective) than HSP90 and very well may represent viable targets for therapeutic intervention using inhibitors. Furthermore, inhibition of a more TPI-selective protein quality control target might be much better tolerated as a TPI Df therapy, which requires chronic and likely life-long administration.

Although we screened for genetic modulators of a mutation that models TPI Df, it is likely that proteins identified will modulate other disease processes. It is common that monogenetic recessive mutations resulting in disease are missense and often subtly impair protein function. It is also not infrequent that pathogenesis results from increased protein turnover, making modulation of protein turnover a potentially attractive therapeutic strategy. Much like protein quality control within the secretory pathway where ~ 1/3 of proteome is expressed has led to considerable investment in the development of therapeutics, cytosolic protein quality control regulating the rest of the proteome is a largely untapped reservoir of possible therapeutic targets. Certainly, proteasome inhibitors have been developed and the ubiquitin system holds considerable promise for drug development (Huang and Dixit, 2016). The identification of additional cytosolic protein quality control proteins, especially small chaperones and previously uncharacterized proteins are important not just as modulators of TPI Df but as drug targets for numerous diseases.

Supplementary Material

Refer to Web version on PubMed Central for supplementary material.

Acknowledgements

We are grateful to the National Institutes of Health for funding this research project (R21 AG059385 and R01 GM103369) and for American Society for Pharmacology and Experimental Therapeutics (ASPET), summer undergraduate research program SURP fellowships that provided support for undergraduate research. We thank Martin Buckley for his thoughtful review of the manuscript. We thank Dr. Enns for assistance obtaining the FB104 patient cell line. We also acknowledge the brave patient and generous parents who donated FB104 cells for biomedical research.

References

Ahner A, Nakatsukasa K, Zhang H, Frizzell RA, Brodsky JL, 2007. Small heat-shock proteins select deltaF508-CFTR for endoplasmic reticulum-associated degradation. Mol. Biol. Cell 18, 806–814. [PubMed: 17182856]

Amor AJ, Castanzo DT, Delany SP, Selechnik DM, van Ooy A, Cameron DM, 2015. The ribosome-associated complex antagonizes prion formation in yeast. Prion 9, 144–164. [PubMed: 25739058]

Andersen RO, Turnbull DW, Johnson EA, Doe CQ, 2012. Sgt1 acts via an LKB1/AMPK pathway to establish cortical polarity in larval neuroblasts. Dev. Biol 363, 258–265. [PubMed: 22248825]

Bengtson MH, Joazeiro CA, 2010. Role of a ribosome-associated E3 ubiquitin ligase in protein quality control. Nature 467, 470–473. [PubMed: 20835226]

Brandman O, Stewart-Ornstein J, Wong D, Larson A, Williams CC, Li GW, Zhou S, King D, Shen PS, Weibezahn J, et al., 2012. A ribosome-bound quality control complex triggers degradation of nascent peptides and signals translation stress. Cell 151, 1042–1054. [PubMed: 23178123]

Brodsky JL, Chiosis G, 2006. Hsp70 molecular chaperones: emerging roles in human disease and identification of small molecule modulators. Curr. Top. Med. Chem 6, 1215–1225. [PubMed: 16842158]

Celotto AM, Frank AC, Seigle JL, Palladino MJ, 2006. Drosophila model of human inherited triosephosphate isomerase deficiency glycolytic enzymopathy. Genetics 174, 1237–1246. [PubMed: 16980388]

Chan HY, Warrick JM, Gray-Board GL, Paulson HL, Bonini NM, 2000. Mechanisms of chaperone suppression of polyglutamine disease: selectivity, synergy and modulation of protein solubility in drosophila. Hum. Mol. Genet 9, 2811–2820. [PubMed: 11092757]

Chinen M, Lei EP, 2017. Drosophila Argonaute2 turnover is regulated by the ubiquitin proteasome pathway. Biochem. Biophys. Res. Commun 483, 951–957. [PubMed: 28087276]

Cox MB, Johnson JL, 2011. The role of p23, Hop, immunophilins, and other co-chaperones in regulating Hsp90 function. In: Molecular Chaperones. Springer, pp. 45–66.

De La Mora-De La Mora I, Torres-Larios A, Mendoza-Hernández G, Enriquez-Flores S, Castillo-Villanueva A, Mendez ST, Garcia-Torres I, Torres-Arroyo A, Gómez-Manzo S, Marcial-Quino J, et al., 2013. The E104D mutation increases the susceptibility of human triosephosphate isomerase to proteolysis. Asymmetric cleavage of the two monomers of the homodimeric enzyme. Biochim. Biophys. Acta 1834, 2702–2711. [PubMed: 24056040]

Defenouillere Q, Yao Y, Mouaikel J, Namane A, Galopier A, Decourty L, Doyen A, Malabat C, Saveanu C, Jacquier A, et al., 2013. Cdc48-associated complex bound to 60S particles is required for the clearance of aberrant translation products. Proc. Natl. Acad. Sci. U. S. A 110, 5046–5051. [PubMed: 23479637]

DiAntonio A, Haghighi AP, Portman SL, Lee JD, Amaranto AM, Goodman CS, 2001. Ubiquitination-dependent mechanisms regulate synaptic growth and function. Nature 412, 449–452. [PubMed: 11473321]

Elefant F, Palter KB, 1999. Tissue-specific expression of dominant negative mutant Drosophila HSC70 causes developmental defects and lethality. Mol. Biol. Cell 10, 2101–2117. [PubMed: 10397752]

Fernandez-Cruz I, Sanchez-Diaz I, Narvaez-Padilla V, Reynaud E, 2020. Rpt2 proteasome subunit reduction causes Parkinson's disease like symptoms in drosophila. IBRO Rep. 9, 65–77. [PubMed: 32715147]

Fogle KJ, Hertzler JI, Shon JH, Palladino MJ, 2016. The ATP-sensitive K channel is seizure protective and required for effective dietary therapy in a model of mitochondrial encephalomyopathy. J. Neurogenet 30, 247–258. [PubMed: 27868454]

Fogle KJ, Smith AR, Satterfield SL, Gutierrez AC, Hertzler JI, McCardell CS, Shon JH, Barile ZJ, Novak MO, Palladino MJ, 2019. Ketogenic and anaplerotic dietary modifications ameliorate seizure activity in Drosophila models of mitochondrial encephalomyopathy and glycolytic enzymopathy. Mol. Genet. Metab 126, 439–447. [PubMed: 30683556]

Genschik P, Sumara I, Lechner E, 2013. The emerging family of CULLIN3-RING ubiquitin ligases (CRL3s): cellular functions and disease implications. EMBO J 32, 2307–2320. [PubMed: 23912815]

Hrizo SL, Palladino MJ, 2010. Hsp70- and Hsp90-mediated proteasomal degradation underlies TPI sugarkill pathogenesis in Drosophila. Neurobiol. Dis 40, 676–683. [PubMed: 20727972]

Hrizo SL, Fisher IJ, Long DR, Hutton JA, Liu Z, Palladino MJ, 2013. Early mitochondrial dysfunction leads to altered redox chemistry underlying pathogenesis of TPI deficiency. Neurobiol. Dis 54, 289–296. [PubMed: 23318931]

Huang X, Dixit VM, 2016. Drugging the undruggables: exploring the ubiquitin system for drug development. Cell Res 26 (4), 484–498. 10.1038/cr.2016.31. Epub 2016 Mar 22. [PubMed: 27002218]

Hunt LC, Stover J, Haugen B, Shaw TI, Li Y, Pagala VR, Finkelstein D, Barton ER, Fan Y, Labelle M, et al., 2019. A key role for the ubiquitin ligase UBR4 in myofiber hypertrophy in drosophila and mice. Cell Rep 28 (1268–1281), e1266.

Ihrig V, Obermann WM, 2017. Identifying inhibitors of the Hsp90-Aha1 protein complex, a potential target to drug cystic fibrosis, by alpha technology. In: SLAS Discovery: Advancing Life Sciences R&D, 22, pp. 923–928. [PubMed: 28346090]

Kudron MM, Victorsen A, Gevirtzman L, Hillier LW, Fisher WW, Vafeados D, Kirkey M, Hammonds AS, Gersch J, Ammouri H, 2018. The modERN resource: genome-wide binding profiles for

hundreds of Drosophila and *Caenorhabditis elegans* transcription factors. Genetics 208, 937–949. [PubMed: 29284660]

Landré V, Rotblat B, Melino S, Bernassola F, Melino G, 2014. Screening for E3-ubiquitin ligase inhibitors: challenges and opportunities. Oncotarget 5, 7988. [PubMed: 25237759]

Lyumkis D, Oliveira dos Passos D, Tahara EB, Webb K, Bennett EJ, Vinterbo S, Potter CS, Carragher B, Joazeiro CA, 2014. Structural basis for translational surveillance by the large ribosomal subunit-associated protein quality control complex. Proc. Natl. Acad. Sci. U. S. A 111, 15981–15986. [PubMed: 25349383]

Mattern MR, Wu J, Nicholson B, 2012. Ubiquitin-based anticancer therapy: carpet bombing with proteasome inhibitors vs surgical strikes with E1, E2, E3, or DUB inhibitors. Biochim. Biophys. Acta 1823, 2014–2021. [PubMed: 22610084]

Miyata Y, 2005. Hsp90 inhibitor geldanamycin and its derivatives as novel cancer chemotherapeutic agents. Curr. Pharm. Des 11, 1131–1138. [PubMed: 15853661]

Murphy ME, 2013. The HSP70 family and cancer. Carcinogenesis 34, 1181–1188. [PubMed: 23563090]

Orosz F, Olah J, Ovadi J, 2006. Triosephosphate isomerase deficiency: facts and doubts. IUBMB Life 58, 703–715. [PubMed: 17424909]

Orosz F, Oláh J, Ovádi J, 2009. Triosephosphate isomerase deficiency: new insights into an enigmatic disease. Biochim. Biophys. Acta 1792, 1168–1174. [PubMed: 19786097]

Pratt WB, Dittmar KD, 1998. Studies with purified chaperones advance the understanding of the mechanism of glucocorticoid receptor–hsp90 heterocomplex assembly. Trends Endocrinol. Metabol 9, 244–252.

Rodríguez-Almazán C, Arreola R, Rodríguez-Larrea D, Aguirre-López B, de Gómez-Puyou MT, Pérez-Montfort R, Costas M, Gómez-Puyou A, Torres-Larios A, 2008. Structural basis of human triosephosphate isomerase deficiency mutation e104d is related to alterations of a conserved water network at the dimer interface. J. Biol. Chem 283, 23254–23263. [PubMed: 18562316]

Roland BP, Stuchul KA, Larsen SB, Amrich CG, Vandemark AP, Celotto AM, Palladino MJ, 2013. Evidence of a triosephosphate isomerase non-catalytic function crucial to behavior and longevity. J. Cell Sci 126, 3151–3158. [PubMed: 23641070]

Roland BP, Richards KR, Hrizo SL, Eicher S, Barile ZJ, Chang TC, Savon G, Bianchi P, Fermo E, Ricerca BM, et al., 2019. Missense variant in TPI1 (Arg189Gln) causes neurologic deficits through structural changes in the triosephosphate isomerase catalytic site and reduced enzyme levels in vivo. Biochim. Biophys. Acta Mol. basis Dis 1865, 2257–2266. [PubMed: 31075491]

Rubenstein EM, Hochstrasser M, 2010. Redundancy and variation in the ubiquitin-mediated proteolytic targeting of a transcription factor. Cell Cycle 9, 4282–4285. [PubMed: 20980825]

Segal J, Mülleder M, Krüger A, Adler T, Scholze-Wittler M, Becker L, Calzada-Wack J, Garrett L, Hölter SM, Rathkolb B, 2019. Low catalytic activity is insufficient to induce disease pathology in triosephosphate isomerase deficiency. J. Inherit. Metab. Dis 42, 839–849. [PubMed: 31111503]

Seigle JL, Celotto AM, Palladino MJ, 2008. Degradation of functional triose phosphate isomerase protein underlies sugarkill pathology. Genetics 179, 855–862. [PubMed: 18458110]

Stewart MD, Ritterhoff T, Klevit RE, Brzovic PS, 2016. E2 enzymes: more than just middle men. Cell Res 26, 423–440. [PubMed: 27002219]

Sun Z, Brodsky JL, 2019. Protein quality control in the secretory pathway. J. Cell Biol 218, 3171–3187. [PubMed: 31537714]

Taldone T, Gozman A, Maharaj R, Chiosis G, 2008. Targeting Hsp90: small-molecule inhibitors and their clinical development. Curr. Opin. Pharmacol 8, 370–374. [PubMed: 18644253]

Torres-Larios A, 2008. Structural basis of human triosephosphate isomerase deficiency. J. Biol. Chem 283, 23254–23263. [PubMed: 18562316]

Wang Y, McAlpine S, 2015. Combining an Hsp70 inhibitor with either an N-or C-terminal Hsp90 inhibitor produces mechanistically distinct phenotypes. Organ. Biomol. Chem 13, 3691–3698.

Yuno A, Lee M-J, Lee S, Tomita Y, Rekhtman D, Moore B, Trepel JB, 2018. Clinical evaluation and biomarker profiling of Hsp90 inhibitors. In: Chaperones. Springer, pp. 423–441.

Zhang Y, Sinning I, Rospert S, 2017. Two chaperones locked in an embrace: structure and function of the ribosome-associated complex RAC. Nat. Struct. Mol. Biol 24, 611–619. [PubMed: 28771464]

Zheng N, Shabek N, 2017. Ubiquitin ligases: structure, function, and regulation. Annu. Rev. Biochem 86, 129–157. [PubMed: 28375744]

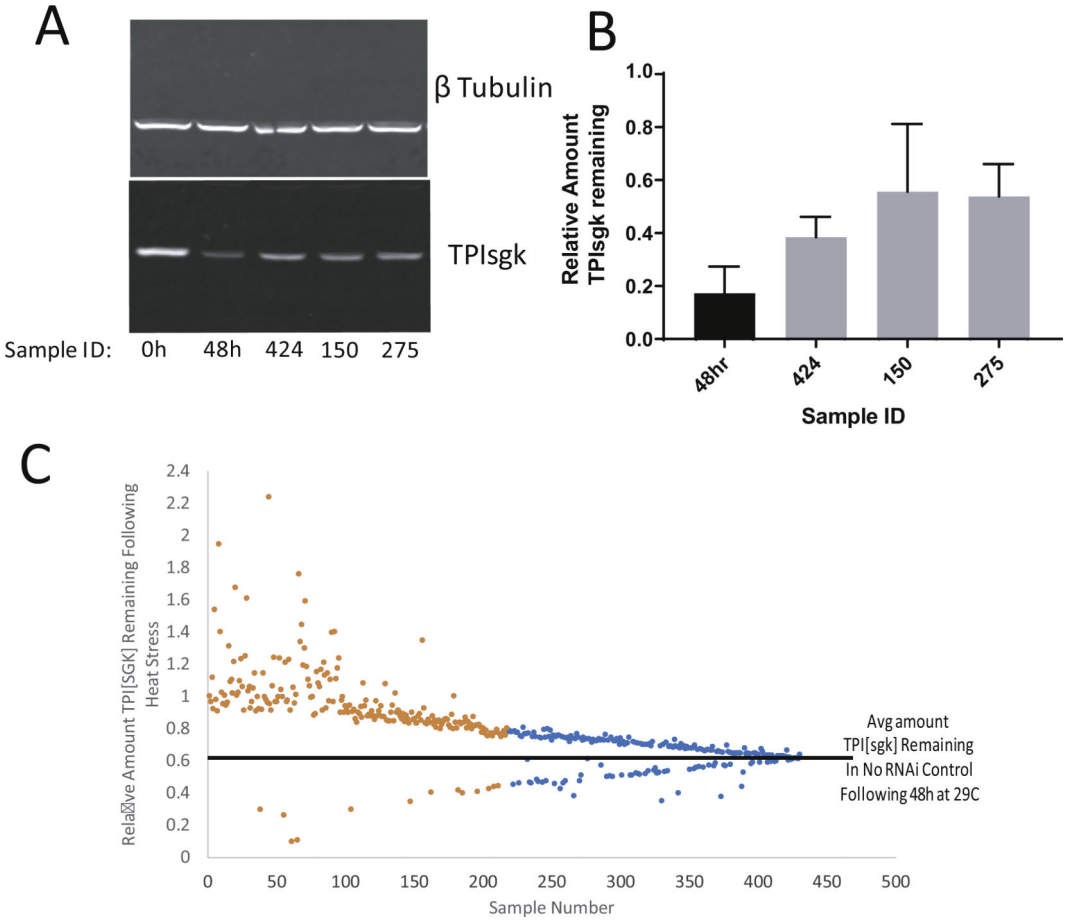

Fig. 1.

RNAi targeting select factors resulted in stabilized levels of TPI^{sugarkill}. The no RNAi samples were reared at 25C (0 h control) and 29C for 48 h were used to determine the relative expected instability of TPI^{sugarkill}. The stability of TPI^{sugarkill} in the RNAi expressing lines was compared to relative TPI^{sugarkill} levels in the RNAi 29C samples on the same blot. For each R line, $n = 4$ sets of Westerns were performed. Panel C: The rescued lines all were significantly different than the 29C TPI^{sugarkill} protein levels by a Student's *t*-test (Orange and Yellow, $p<0.05$). A Bonferroni post-test was performed (Yellow only, $p<0.00011$). Error bars in panel B represent SEM. The samples that were initially identified as potential factors involved in TPI^{sugarkill} turnover were selected for a second round of screening (orange and yellow). The identity of the factors shown in Panel A and B are as follows: 424 (CG4599, TPR 2), 150 (CG8937, Hsp70), 275 (CG12161, Proteasome b2 Subunit 2).

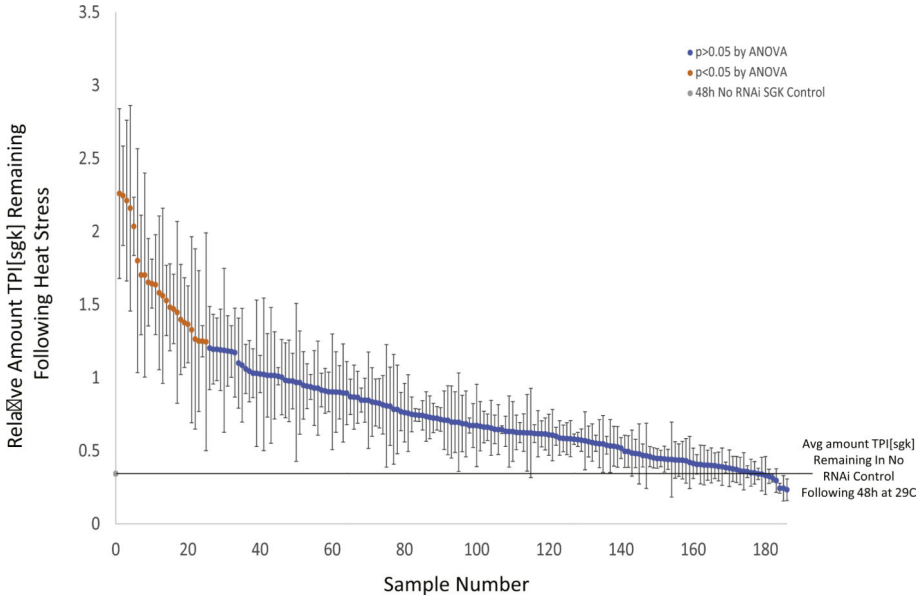

Fig. 2.

Secondary round of screening identified 25 potential regulators of $TPI^{sugarkill}$ degradation. The no RNAi samples reared at 25C (0 h control) and 29C for 48 h were used to determine the relative expected instability of $TPI^{sugarkill}$. The stability of $TPI^{sugarkill}$ in the RNAi expressing lines was compared to relative $TPI^{sugarkill}$ levels in the RNAi 29C samples on the same blot. For each RNAi line, n = 4 sets of Westerns were performed. Samples were compared to the no RNAi 48 h 29C control set by a One-Way ANOVA with a Dunnett's Post Test (Blue: $p>0.05$, Orange: $p<0.05$).

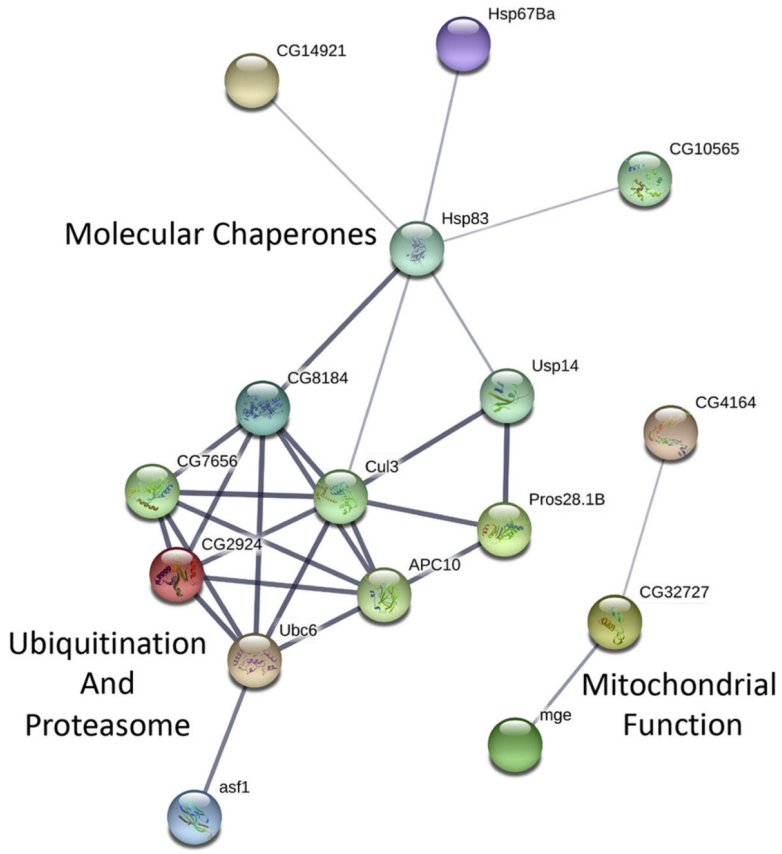

Fig. 3.

Chaperones and protein degradation regulators are enriched in the hits from both rounds of screening. A STRING network was developed by evaluating the genes identified in 2 rounds of western blot screening of RNAi samples. The interactions were assessed as follows experimental evidence, database evidence, co-expression data, text mining data and co-occurrence. Thickness of lines indicates strength of evidence for interaction.

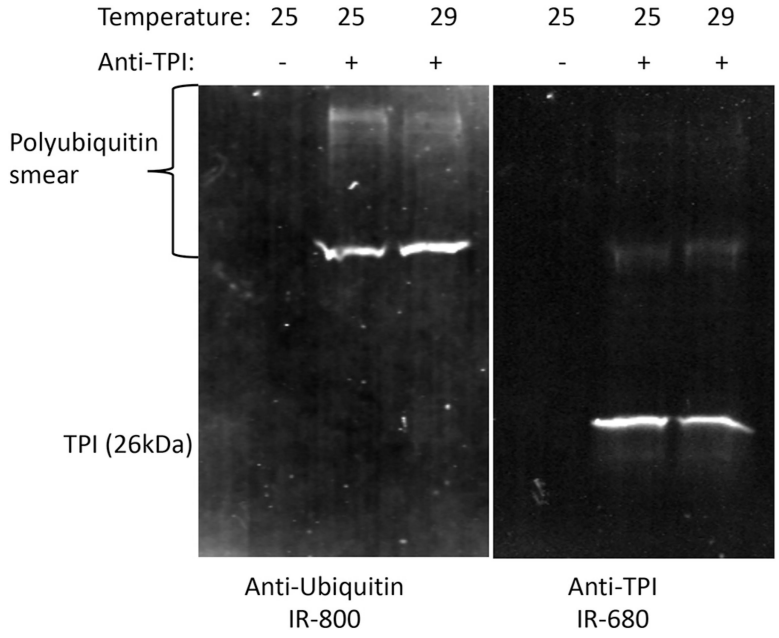

Fig. 4.

TPI^{sugarkill} is polyubiquitinated. Flies treated with MG132 for 24 h and incubated at either 25 or 29C were homogenized and TPI^{sugarkill} was immunoprecipitated with anti-TPI. A bead only negative control was included. The characteristic polyubiquitin smear is visible in the samples with immunoprecipitated TPI^{sugarkill} protein.

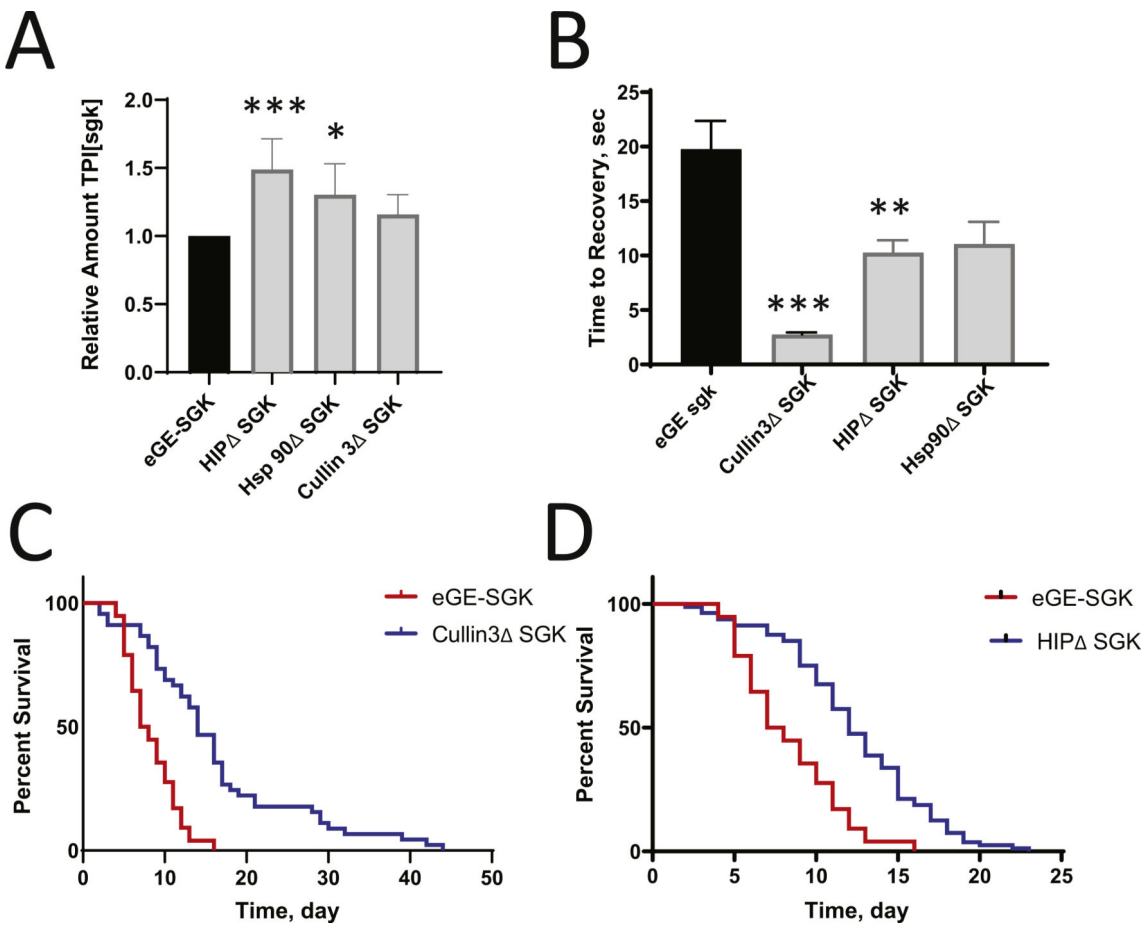

Fig. 5.

Knock down of Cullin 3, HIP and Hsp90 with p-element disruption results in increased $TPI^{sugarkill}$ protein levels that correlates to extended lifespan and reduced bang sensitivity in $TPI^{sugarkill}$ homozygotes. P elements were used to disrupt the expression of genes (cullin 3, Hsp90 and HiP). Flies were homozygous for both the p-element disruption and the $TPI^{sugarkill}$ allele. A) Western blots were performed following incubation of flies at 25C for 5 days and compared to a $TPI^{sugarkill}$ homozygote control incubated at the same time. One-way ANOVA analysis was used to determine significance (* $p<0.05$). Error bars are SEM. B) Mechanical stress sensitivity assays were completed on flies reared at 25C. For HIP analysis ($n = 50$). For Cullin 3 analysis ($n= 30$). For Hsp90 analysis ($n = 25$). Average time to recovery was calculated and compared to a $TPI^{sugarkill}$ homozygote by One-way ANOVA analysis for each p element line (* $p<0.05$, ** $p<0.01$ and *** $p<0.001$) Error bars show are SEM. C and D) Lifespans were completed in triplicate with approximately 25 flies per vial at 25C. Survival curves and median lifespan were compared to a $TPI^{sugarkill}$ homozygote control using PRISM software for each p element line.

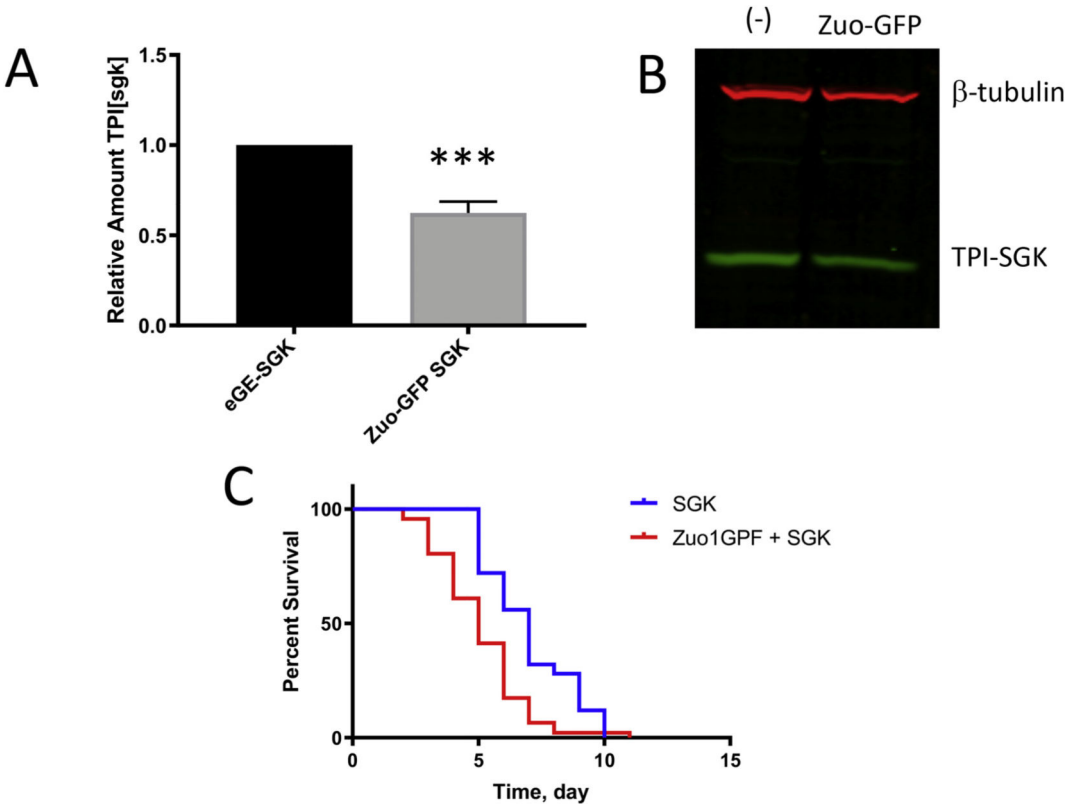

Fig. 6.

Overexpression of the RAC associated HSP40 (Zuo1) results in TPI^{sugarkill} destabilization and reduced lifespan. A. Western blots were conducted following a 29C temperature shift for 48 h on TPI^{sugarkill} homozygotes with and without an extra copy of Zuo1-GFP for increased expression. Densitometry was completed using Image J and the results were analyzed for significance by Student's *t*-test ($n = 7$, $P<0.0001$). Error bars shown are SEM. B) A representative image from the western blot analysis is shown. C) The TPI^{sugarkill} flies overexpressing Zuo1-GFP were compared to a TPI^{sugarkill} homozygote control and found to have a reduced lifespan by analysis with PRISM software (5 day median lifespan, compared to the 7 day median lifespan observed in TPI^{sugarkill} flies, $p<0.05$).

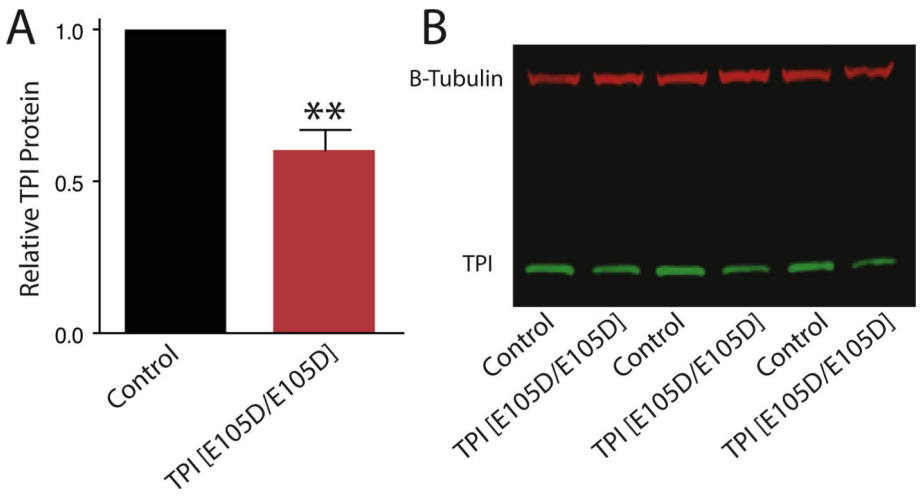

Fig. 7.

E105D TPI is unstable compared to wildtype TPI protein in human fibroblasts. Total TPI protein levels were compared by Western blot (WB) between extracts from wild type control and patient (*TPI*$^{E105D/E105D}$) fibroblasts (FB104). Panel (A) quantifies the WB data shown in panel (B). Beta-tubulin was used as a loading control for the WB analysis. TPI protein in patient cells was significantly reduced compared to the control when assessed using a Student's *t*-test (** $p<0.01$, $N=3$).

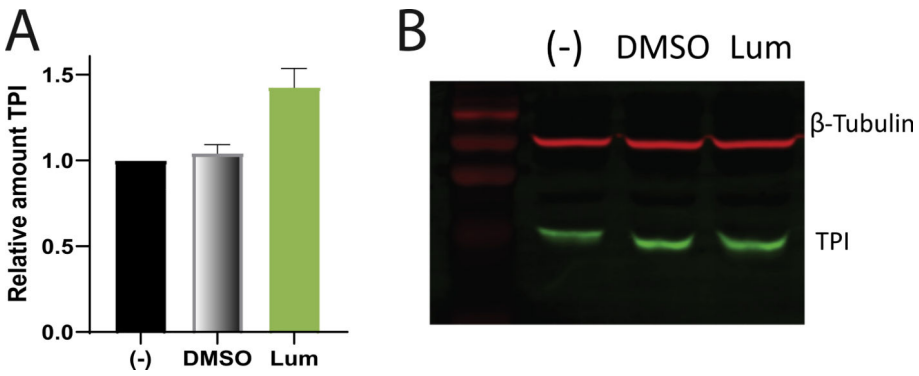

Fig. 8.

Treatment with the Hsp90 Inhibitor, Luminespib, results in an increase in TPI levels in patient $TPI^{E105D/E105D}$ fibroblasts. A. Densitometry was completed on Western blots and the results were analyzed for significance by Student's t-test ($n = 4$, $^{**}P<0.01$). Error bars shown are SEM. B) A representative western blot was conducted following treatment of patient line FB104 with 200 nM Luminespib for 48 h. at 37C.

Table 1

Genes identified as potential regulators of TPI degradation.

R#	ANOVAp value	CG#	Function	Closest human ortholog via DIOPT v8.0
36	<0.0001	CG4167	Heat Shock Gene 67Ba	Hspb1
62	0.0001	CG1662	*Unknown Function* Proposed Role in Mitochondial Ribosome Assembly	MGC12972
94	0.0262	CG10565	*Unknown Function* (Hsp40 proposed component of RAC, Zuo1)	DNAJC2
119	0.0028	CG11419	Anaphase Promoting Complex Subunit 10	APC subunit 10
161	<0.0001	CG2924	*Unknown Function* Proposed E2 ubiquitin-conjugating enzyme	UBE2Q1
212	0.0203	CG2013	Ubc6, E2 Ubiquitin Conjugating Enzyme	UBE2B
215	0.0257	CG14981	Maggie, Mitochondrial Transporting ATPase	TOMM22
220	0.0107	CG14921	*Unknown Function* Proposed Hsp20	DNAAF4
255	<0.0001	CG1242	Heat Shock Protein 83	HSP90-A2
307	<0.0001	CG7225	Windbeutel, Toll Signaling in Golgi	ERP29
314	<0.0001	CG8560	*Unknown Function* Proposed metallocarboxypeptidase activity	CPB1
347	<0.0001	CG8184	HUWE1, E3 Ubiquiting protein ligase	HUWE1
315	<0.0001	CG5116	*Unknown Function* Proposed ribosome binding activity	GTPBP6
359	<0.0001	CG4569	Proteasome alpha 4 Subunit	PSMA7
361	0.0004	CG7558	Arp3 (Actin Related Protein)	ACTR3
374	<0.0001	CG4165	Ubiquitin Specific Protease 16/45	USP45 and USP16
375	0.0004	CG8860	*Unknown Function* Proposed Translocon Activity	Sec61G
397	<0.0001	CG4461	*Unknown Function* Proposed Hsp20	CRYAA
398	<0.0001	CG7656	*Unknown Function* Proposed E2 ubiquitin-conjugating enzyme	CDC34
399	<0.0001	CG42616	Cullin 3, Ubiquitin Conjugating Enzyme Binding	CUL3
411	<0.0001	CG7220	*Unknown Function* Proposed E2 ubiquitin-conjugating enzyme	UBE2W
421	0.0018	CG32727	*Unknown Function* Proposed Hsp40	DNAJC15
435	0.0279	CG6342	IRP1-B, Aconitase	ACO1
455	0.0035	CG4164	Shriveled, Hsp40	DNAJB11
504	0.0068	CG9383	Anti-silencing factor 1	ASAF1A